GEOLOGICAL MODEL AND PERMEABILITY FRAMEWORK OF BUKIT DAUN GEOTHERMAL FIELD, INDONESIA

Muhammad Ikhwan[1], Irene C Wallis[2] and Julie V Rowland[2]

[1] Pertamina Geothermal Energy, Skyline Building Level 19th, Jalan M. H. Thamrin No.9, Jakarta, Indonesia

[2] School of Environment, University of Auckland, 23 Symond Street, Auckland Central, New Zealand

ikhwan.aziz@pertamina.com

Keywords: *Bukit Daun, Sumatra, exploration, geology and structural modelling, borehole image logs, permeability.*

ABSTRACT

We present results from a study that investigates the geological setting of Bukit Daun geothermal field, Indonesia and how that geology may influence hydrology. Our analysis addresses geologic controls from the regional to the wellbore scale, and incorporates data provided by Pertamina Geothermal Energy with publicly available terrain images and geologic data. Extensive use of the regional geologic setting (i.e., outside the prospect area) enabled us to improve the confidence and plausibility of the geologic interpretation.

We developed a 3D geologic and structural model and used it as a framework for a hydrologic interpretation that is based on well temperature profiles, feedzone locations, distribution of surface manifestations, and shape of the clay cap. Pertamina Geothermal Energy's drilling success discovered a potentially viable resource and our study proposes a hydrologic model for that resource. Our analysis identifies those elements of the geology that may influence fluid flow at the reservoir and wellbore scale.

1. INTRODUCTION

The Bukit Daun geothermal field is located in southern Sumatra within the Bengkulu province, about 60 km to the northeast of the province capital Bengkulu (Figure 1A). This prospect is associated with volcanic centres and the Sumatra Fault System (SFS). The SFS is a segmented and sinuous right-lateral, strike-slip fault zone that accommodates up to 6 mm/yr of oblique convergence between the Indo-Australian and Eurasian plates (Bellier and Sébrier, 1994).

Bukit Daun is located between the southern tips of two adjacent segments of the SFS (the Musi and Ketahun segments) that were identified by Sieh and Natawidjaja, (2000) using topographic analysis (Figure 1A). A Holocene volcanic field is located between these fault segments. Although Sieh & Natawidjaja, (2000) propose a releasing 6-8 km stepover zone between these segments, the degree of interaction is unclear because surface evidence is obscured by young volcanic deposits. As will be shown in our DEM analysis, surface structures that cut the Quaternary deposits at Bukit Daun are coherent with local SFS geodynamics.

The geology of South Sumatra is divided into four geologic-physiographic zones generated by the Paleogene onset of subduction (Kusnama et al., 1992). The Bukit Daun field is located between the Bengkulu Basin zone (blue) and the Bukit Barisan zone (triangle, Figure 1B).

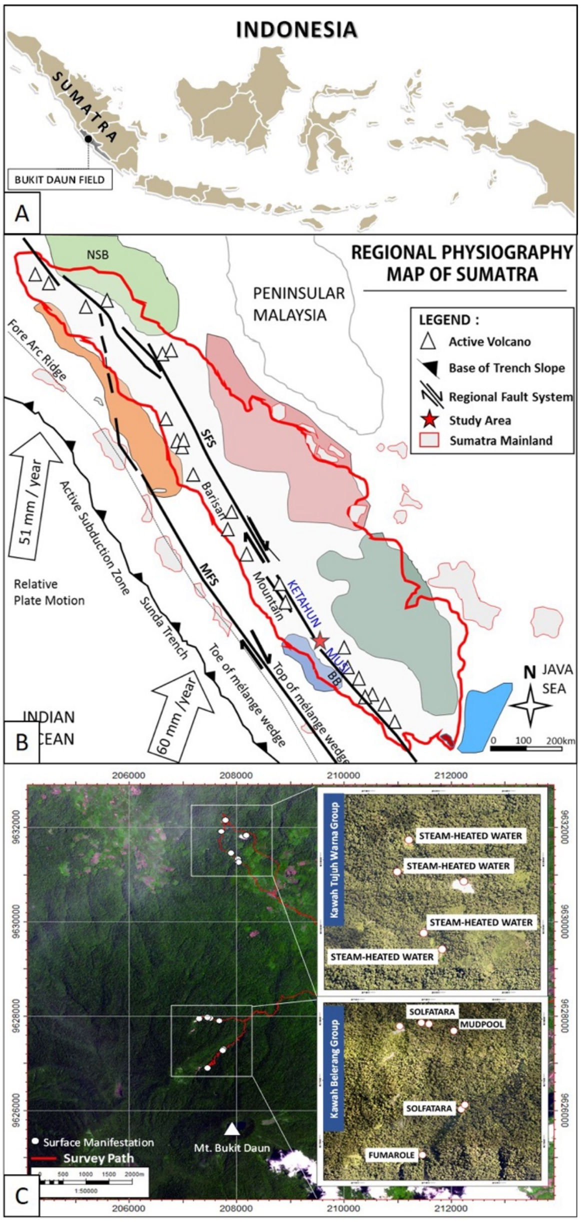

Figure 1: (A) The regional context of Bukit Daun. (B) Bukit Daun plotted with key geologic-physiographic features in Sumatra (after Moore and Curray, 1980; Darman and Sidi, 2000) where BB = Bengkulu Basin, SFS = Sumatra Fault System, and MFS = Mentawai Fault System. (C) Distribution of thermal manifestations at Bukit Daun geothermal field.

The Bengkulu basin, a forearc basin, consists of a turbidite sequence which records a marine transgression that initiated during the mid-Miocene (Barber et al., 2005). Yulihanto et al. (1995) propose that this basin formed as a result of interaction between the SFS segments with uniform kinematic movement (i.e., right-lateral strike-slip faults). The presence of tuffaceous material in mid-Miocene sediments points to active volcanism during this period, but the source is uncertain. The Bukit Barisan zone, which includes the Barisan Mountains, is dominated by the products of arc volcanism. This arc volcanism commenced in the Oligocene to mid-Miocene and continues through to the present day.

Two groups of surface manifestations indicated the presence of a geothermal resource at Bukit Daun. One group consists of fumaroles, solfatara, mudpools near the crater. A second group lies ~3 km down the flank of Bukit Daun and consists of steam-heated waters (Figure 1C). PT. Pertamina Geothermal Energy (PGE) drilled three exploration wells at Bukit Daun in 2016 that intersected a viable high-temperature geothermal resource with benign fluids. In this paper we present results from a study that combines data from that drilling campaign with publicly available data to generate a geologic model of Bukit Daun and consider geologic controls on fluid flow at the well- and reservoir-scale (Ikhwan, 2020). We will describe our interpretation of the stratigraphic and structural setting that was used to generate a 3D geologic model. Then we describe what is known about the geothermal system, which is based on well testing, geophysics and surface manifestations, and compare it to the geologic framework. From this, we propose a set of mechanisms that may control fluid flow at Bukit Daun. Understanding the geologic controls on fluid flow will benefit future well targeting and the development of the conceptual model at Bukit Daun.

2. GEOLOGICAL SETTING

2.1 Stratigraphy

Due to its location between the Bengkulu Basin and the Barisan Mountains, the stratigraphy at Bukit Daun contains both sedimentary and volcanic deposits. Drilling and surface mapping have confirmed the presence of Neogene-Paleogene metasedimentary deposits interlayered with volcanic deposits below an > 3 ma erosional unconformity, referred to herein as the orogenic unconformity. Quaternary lava and pyroclastic products are present above this unconformity. At surface, the Bukit Daun geothermal field is dominated by a stratovolcanic centre with geomorphic evidence for multiple eruptive vents and flows. Much of the geothermal field is covered by Quaternary volcanic products (Figure 2) but the reservoir rocks are located below the unconformity in Cretaceous to Neogene aged formations.

2.1.1 Surface Stratigraphy

The oldest formation mapped at surface, Hulusimpang Formation (Tomh), was deposited during the late Oligocene to early Miocene (Gafoer et al., 1992). It is characterized by various volcanic-sedimentary products, including andesite lava, volcanic breccia, lahar deposit, tuffs, and lapilli. It dominates the north and eastern area of Bukit Daun. Seblat Formation (Toms) comprises tuffaceous and volcanic-sedimentary material and is exposed in the southern part of the field. Some younger Neogene deposits are also mapped at surface, such as Bal Formation (Tmba), Senayan Formation (Tpan), and Kemumu Formation (Tmak). These Neogene-Paleogene deposits were eroded during the orogenic period, and their eruption centers are unknown. However, deposition of the Hulusimpang Formation is attributed to a period of highly productive pre-Quaternary volcanism with widespread coverage (Barber et al., 2005). In contrast to the pre-Quaternary metasedimentary deposits identified in the subsurface at Bukit Daun, there are no marine sediments in the Quaternary deposits cropping out at surface (Kusnama et al. 1992).

The Bukit Daun stratovolcanic center includes several Quaternary volcanic domes. Circular features associated with these domes are mapped in the vicinity of the Mt. Bukit Daun eruption centers and include Mt. Hulupalik, Mt. Bengkuang, Mt. Tiga, Mt. Hulukokai, and Mt. Aning (Ikhwan, 2020). As these Quaternary volcanoes have similar petrology and their eruption may have overlapped in time and space, the stratigraphic reconstruction is challenging (McCarthy et al., 1992).

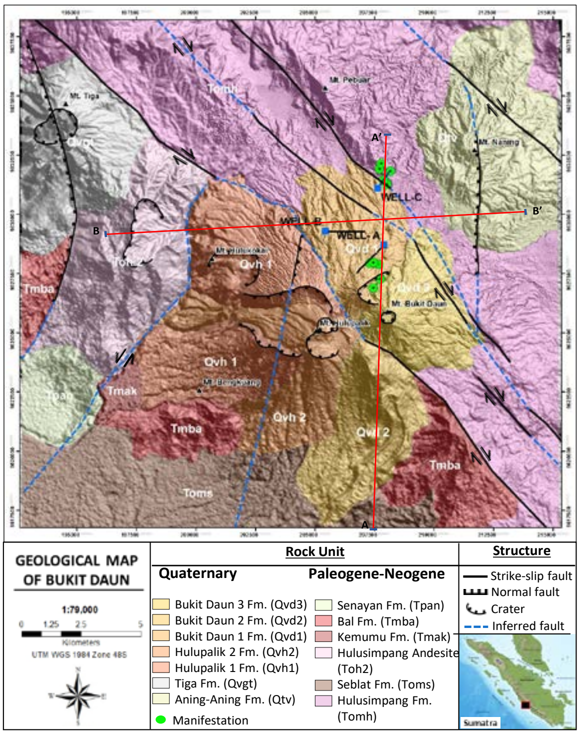

Figure 2: The geological map of the Bukit Daun field that we refined by using the LiDAR and DEM images (key for the map is shown in Table 1). Red lines mark the position of cross-sections in Figures 3 and 8.

2.1.2 Subsurface Stratigraphy

We interpreted data from three exploration wells, Well-A, Well-B, and Well-C, in the context of regional geology to generate the subsurface stratigraphy (see Figure 2 for locations and Figure 3 for the well sections). At reservoir depth, formation boundaries and lithology are constrained by cuttings, conventional and sidewall core, drilling parameters, and micro-resistivity borehole image log interpretation. Well-A intersected Bukit Daun 1, Hulupalik 2, and Hulusimpang, Kikim, and Saling Formations. Hulupalik 2 Formation unconformably overlies the Hulusimpang Formation. The unconformity between Quaternary and Neogene formations in Well-A likely coincides with this contact. Kikim is the oldest Paleogene unit in the Bukit Daun and is dominated by welded tuff. Sedimentary material in the

Kikim Formation records the development of rift basins during what Barber et al., (2005) refers to as the 'horst-and-graben stage'. The Kikim Formation unconformably contacts the Cretaceous basement, the Saling Formation. This basement primarily consists of lava and tuff and the cuttings and core samples contain abundant secondary epidote and chlorite. It was folded and uplifted during the late Cretaceous, rifted in association with subsequent basin development, and uplifted again in response to the current subduction regime (McCarthy & Elders, 2014). A diorite intrusion was identified in a conventional core sample in well-A, and it intrudes the Kikim formation at 2170 mMD. However, the thickness of this intrusion still unknown and it has not yet been age dated.

Well-B was drilled near Well-A, and the stratigraphy is similar. From surface to the production casing point, Well-B penetrates Bukit Daun 1, Hulupalik 2, Hulupalik 1, and Hulusimpang Formation. In this well, we interpret the contact between Hulupalik 1 and Hulusimpang Formation as the Neogene-Quaternary orogenic unconformity. This unconformity occurs at a similar elevation in Well-B and Well-A. Cutting samples from 1501, 2002, and 2101 mMD included metasedimentary material with abundant microfossils (PGE unpublished report, 2015). Three foraminifera species were recognized based on characteristics defined by Bolli & Saunders (1989) and Postuma (1971): Globigerinoides primordius (late Oligocene to early Miocene) in Hulusimpang Formation, Globigerina praebulloides praebulloides (late Eocene to middle Miocene) in Kikim Formation, and Globigerina ciperoensis ciperoensis (middle Oligocene) in Kikim Formation. Each species indicates an age range that broadly matches the suggested formation age in which they were found (Table 1).

Well-C penetrates Bukit Daun 1 Formation, which is dominated by tuff and volcanic breccia. Core and micro-resistivity borehole image log were not acquired in this well, so the geologic interpretation is lower confidence and resolution than Well-A and Well-B. Nevertheless, we were able to infer that the orogenic unconformity is present near-surface because Bukit Daun 1 is intersected shallow in the well and the Hulusimpang formation is exposed just north of the well pad (cross section A-A'). Although Well-C is shallowest of the three exploration wells, it penetrated the Kikim and Saling formation because these basement rocks are shallowest in the northeast of Bukit Daun.

2.2 Structure

Surface structural analysis without 'boots on the ground' observation points typically have high uncertainty. Although field survey was beyond the scope of the present work, it would have only marginally reduced uncertainty because dense jungle and deep weathering profiles obscure the surface geology at Bukit Daun. We sort to reduce uncertainty associated with existing maps of surface structure and improve on these models though: (1) judicious application of remotely-acquired terrain images (LiDAR and IFSAR), (2) integration with micro-resistivity borehole images data that reveals reservoir-depth structural trends, and (3) by ensuring the proposed structural model is coherent with the structural-tectonic setting of Bukit Daun. The main structural features are plotted in Figure 4 and described below.

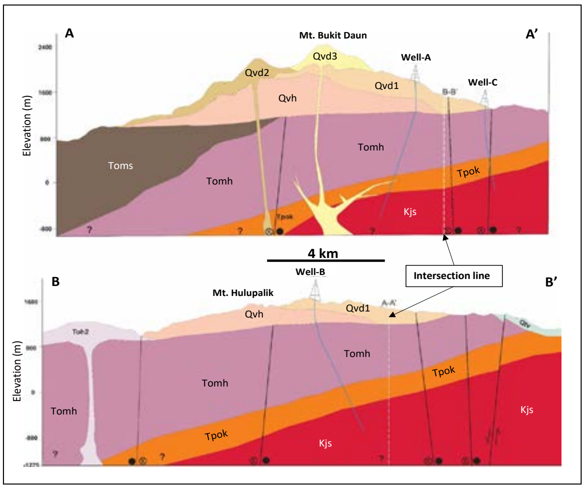

Figure 3: Cross-sections generated using surface and well data. Pre-Quaternary formations tilt and are likely part of a system of folds that have a NW-SE axis associated with orogenic phase of compression. Quaternary volcanism sits unconformably on the eroded unconformity. Section locations are in Figure 2. The key for these sections is Table 1 where the geologic sequence is described.

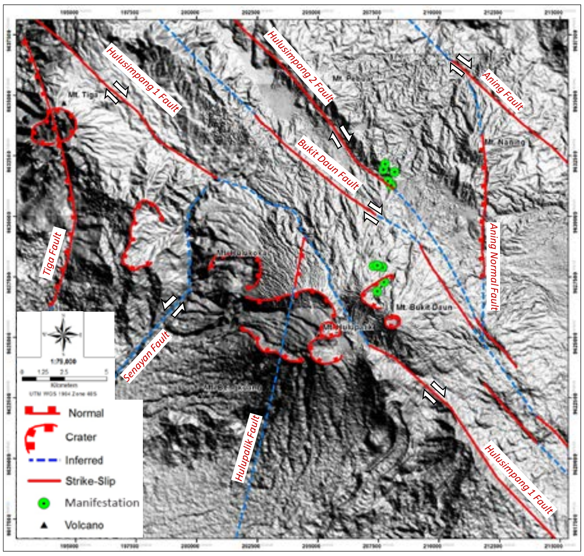

Figure 4: Mapped major faults and craters in the local Bukit Daun area. Features in red are high-confidence faults or craters, while the blue dashed lines are inferred faults. Most surface faults are parallel or sub-parallel to the SFS.

Table 1: Stratigraphic column for Bukit Daun that combines mapped and described surface deposits with regional tectonic and stratigraphic stages (modified after Gafoer et al. 1992)

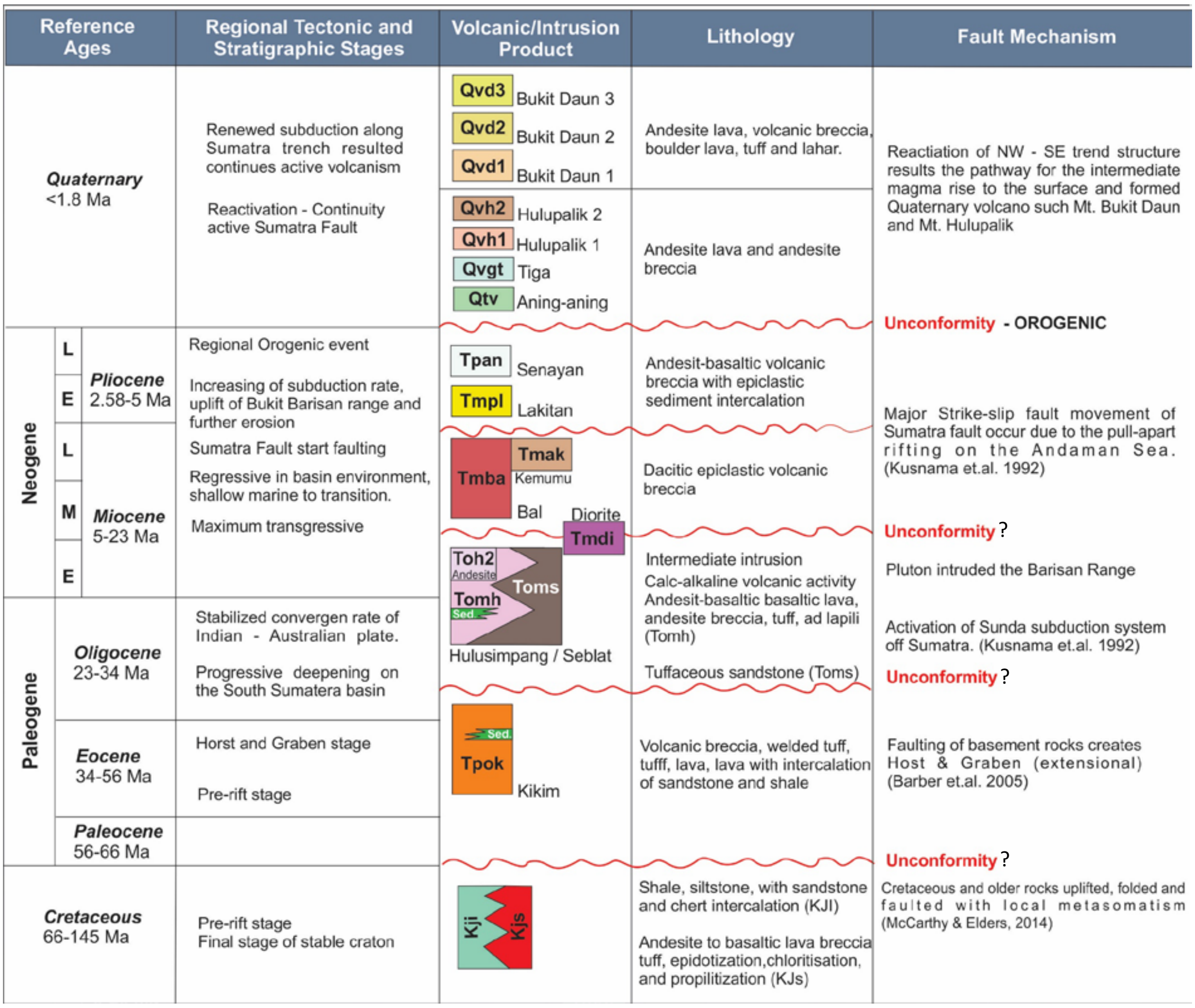

2.2.1 Surface Structure

Surface image analysis indicates that Bukit Daun geothermal field is controlled at the regional scale by two right-stepping NW–SE right-lateral striking strike-slip faults associated with the SFS (Ketahun and Musi segments: Figure 1A). Within the local Bukit Daun area (Figure 4), we inferred surface faults by combining lineament and volcano-stratigraphy analysis of terrain images. The local fault pattern is consistent with, and thus can be interpreted based on, a Riedel simple shear model. A Riedel simple shear model is consistent with the regional context. In this model, mapped N-S striking faults are the likely the result of extension directed toward 135°. Examples include the Tiga and Aning Faults, which are included in the 3D geologic model (Figure 6). NW–SE striking faults are classified as either: (1) "Old" NW–SE striking faults, which have not displaced Quaternary deposits or (2) "Young" NW–SE striking faults, which have cut Quaternary deposits. The northern group of geothermal manifestations appears to be controlled by an old NW–SE striking fault (Hulusimpang 2 Fault), while the group appears to be localized around Mt. Bukit Daun and possible sector collapse.

2.2.2 Subsurface Structure

We used image logs acquired in the production interval of Well-A and Well-B to improve our understating of subsurface structure. Figure 5 plots the orientation of fractures imaged in each formation. The subsurface structural architecture is varied, but N-striking orientations are dominant (Figure 5A). These subsurface fracture trends contrast with those defined at surface, where the latter of which dominantly show NW-striking structures parallel with the SFS. The dominance of N-striking fracture may be due to geometric sample bias generated by the eastward and southwest well deviations (c.f., Wallis et al. this volume).

In geothermal systems elsewhere, homogeneous rocks show more consistent structural orientations (Wallis et al., 2015) and lithology impacts fracture frequency (Wallis et al. this volume, Masri et al. 2015). Similar patterns in fracture orientation and frequency were observed at Bukit Daun. Based on wellbore image interpretations and their correlation with other datasets, we can make the following observations:

- Abundant electrically conductive fractures are present, and these fractures may be either open (water filled) or filled with conductive minerals (e.g., clay or pyrite).
- The dominant fracture trends in the borehole images (NW–SE, N–S, W–E, and NE–S) are consistent with the structural trends identified at surface or in the regional geologic context.
- NW–SE striking fractures dominate in the Paleogene-Neogene aged Hulusimpang Formation (Figure 5A). This trend is consistent with the SFS, which has been active from Miocene-to-recent and may reflect either reactivation of old fractures or generation of new fractures.

- N–S trending fractures dominate below 2057 mMD in Well-A. NE-SW and NW-SE striking (SFS-parallel) fractures were imaged but are less numerious (Figure 5A). Relic N-S and NE-SW faults may be present below the orogenic unconformity, perhaps associated with the Bengkulu Basin graben system that comprises NE-SW (Paleogene Graben) and N-S (Neogene Graben) striking normal faults. The Bengkulu Basin formed between the SFS and MFS, in a right-lateral fault stepover. One of the Neogene N-S normal faults, the Napalan Fault, is thought to cross beneath the Bukit Daun volcano (Yuliharto et al., 1995). However, the relative dominance of north-trending fractures may be enhanced by geometric sample bias. Further work is required to establish the dominant fracture trends in the reservoir without geometric bias and to evaluate the likelihood that deep N-S faults are active (open to fluid flow) given current tectonic setting and relic structural architecture.

2.3 3D Geological Model

To build the 3D geologic model, the 2D cross-sections (e.g., Figure 3) were geo-referenced together with the results of structural and volcano-stratigraphic interpretation of topographic images. These were used to generate a plausible 3D geologic model beyond the limited spatial coverage provided by well data (Figure 6).

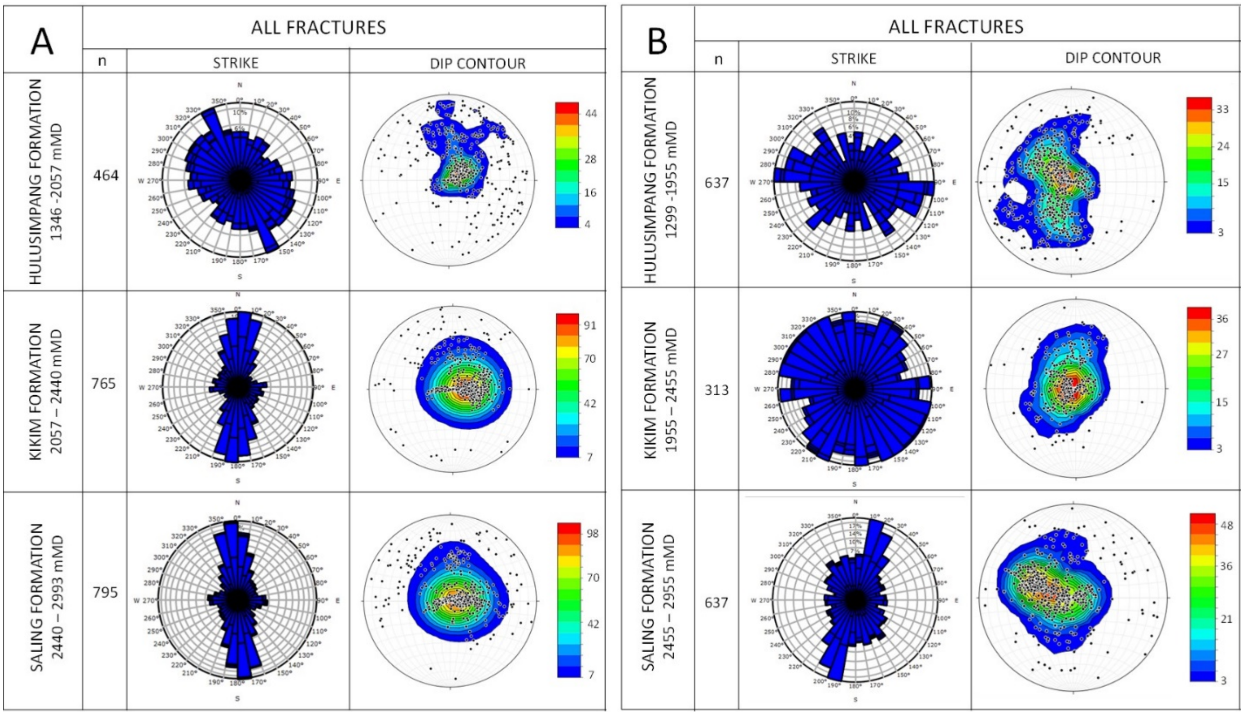

Figure 5: (A) Fracture trends for each formation in Well-A. (B) Fracture trends for each formation in Well-B. The consistent N-striking and NE-striking fracture sets imaged in the boreholes are absent on the surface.

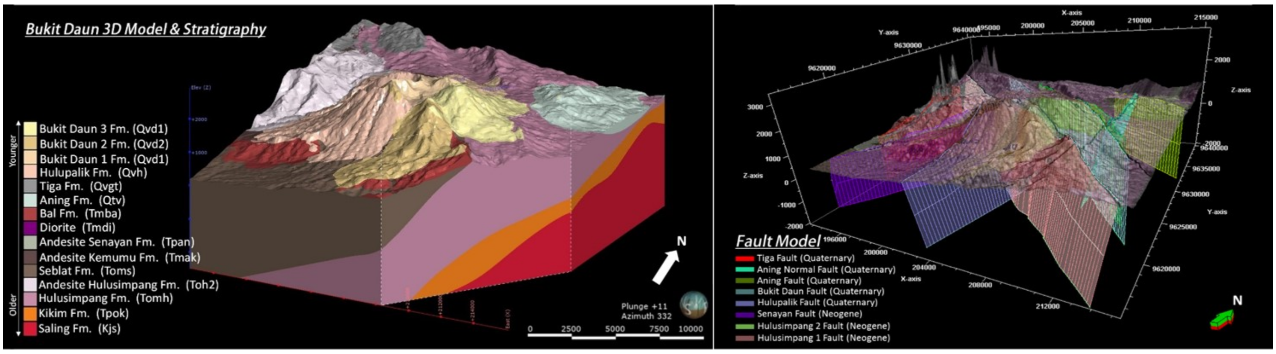

Figure 6: 3D stratigraphy (left) and fault model (right) of the Bukit Daun geothermal field. The geologic model is 10 km² in the horizontal dimension and spans 2000 to 3000 mRSL in the vertical dimension. The stratigraphy model is sliced in a NE-SW direction to illustrate the geologic dip below the orogenic unconformity.

3. GEOTHERMAL SYSTEM OF BUKIT DAUN

Bukit Daun geothermal field is a neutral, volcanic-hosted geothermal system with an upflow in the south near Well-A and a north-northeast outflow past Well-C. In this section, we provide evidence for our interpretation of the upflow-outflow arrangement and the following section outlines geologic mechanisms that may control that arrangement. The fluid flow hypothesis reflected by the isotherms in Figures 7 and 8 is a simple upflow-outflow model and does not imply a probabilistic resource volume (Cumming 2016). Given the presence of young volcanic cones and solfatara in the southern cluster of thermal manifestations, Bukit Daun may have an associated vapour core. This alternative conceptual model is not reflected in the isotherms presented here. Other alternative conceptual models, particularly in terms of reservoir volume (width and thickness), may also fit the available exploration data (Wallis et al. 2017).

An upflow on the northern flank of Bukit Daun is strongly suggested by the presence of solfatara and fumarole (Kawah Belerang group). Well-A is deviated under these thermal manifestations. It is the hottest of the three exploration wells (~260°C) and is isothermal from -650 (terminal depth) to 350 mRSL where it meets the BPD curve. Well-A has the highest injectivity of the three exploration wells (32.7 t/hr.bar). In our model, the hot liquid rises buoyantly to the north and the steam phase ascends directly through the low-resistivity clay cap to the Kawah Belerang thermal manifestations. The rising steam is likely responsible for the dome shape in the base of the clay cap at and south of Well-A.

Mudpools and sulfate hot springs (Tujuh Warna group) are present down the northern flank of Bukit Daun volcano and are likely related to the outflow. Well-C is the second most permeable well (15.9 t/hr.bar) and is deviated under this group of thermal manifestations. As would be expected on the outflow path, it is cooler (~210°C) and includes a ~10°C inversion at depth. The sulfate hot springs in the outflow zone may reflect perched, steam-heated meteoric water (PGE unpublished reports, 2015). The absence of chloride hot springs in the outflow zone may be the consequence of a deep watertable. Well-B is between Well-A and Well-C but is closer to the former. It has the lowest injectvitiy (11.4 t/hr.bar) and the presence of interzonal flows in Well-B makes it difficult to confidently determine the reservoir condition. However, the stable bottom-hole temperature is ~260°C (-700 mRSL), so it appears to penetrate the northward outflow path from Well-A to Well-C (Figure 7B).

4. PERMEABILITY FRAMEWORK

Although a range of conceptual models may be generated to fit the exploration data, the general location of the upflow and the outflow direction are constrained. Consequently, our investigation into the geologic mechanisms controlling reservoir-scale fluid flow focuses on these.

4.1 Upflow

Spatial comparison between the system, as described above, and our structural model indicates that the upflow may be controlled by N-S relic faults (i.e., Neogene Napalan Fault) and NNW-SSE structures, which are the dominant fracture patterns in Well-A. As discussed in Section 2.2, the north-trending structure imaged in wells below the orogenic unconformity were not visible in the terrain image analysis because they are covered by the Quaternary volcanic deposits. Faulting associated with the SFS dominates at surface. It is possible, however, that interaction between relic structure and more recently active faults have a generated complex, connected permeability network.

4.2 Outflow

We identified three possible geologic mechanisms that could influence fluid flow on the outflow (Figure 8):

1. Faults responsible for the N-S dominant fracture trend in Well-A may propagate northward toward the Tujuh Warna group of thermal manifestations.
2. Based on comparison between high-resolution lithology data interpreted from the micro-resistivity borehole image and the completion test data, the volcanic breccia within the Hulusimpang Formation in Well-A has high permeability. The image log in Well-B, which has the lowest injectivity, revealed this well does not intersect the Hulusimpang Formation volcanic breccia. Well-C has no borehole image data to allow recognition of this lithology type. The Hulusimpang Formation crops out to the north and south of Bukit Daun, so this permeable volcanic breccia may be extensive.
3. Buoyant fluid may flow up-dip within the tilted pre-Quaternary formations and, depending on the relative permeabilities, flow may occur preferentially within some units (e.g., the Hulusimpang Formation volcanic breccia).

4.3 Reservoir Extent

We evaluated the shape of the clay cap, specifically the thickening/deepening of the conductive zone imaged by MT, in conjunction with our geologic model to explore possible geologic controls on the northeast and eastern extents of the reservoir. The nature of the western boundary remains unclear.

The NW-SE striking Hulusimpang 2 fault appears to influence hydrology at the limits of the outflow (Figure 8). The presence of the Hulusimpang 2 is inferred from large-scale surface lineaments identified in LiDAR imagery, but the kinematics and dip direction are equivocal. The thermal manifestations of the Tujuh Warna group align on this structure, which indicates that it may play a role in enhancing vertical permeability. In contrast, the Kawah Belerang group has no obvious structural control.

The clay cap dips steeply and thickens on the east side of Hulusimpang 2. As shown in Figure 7A, the outflow may turn at this point from a generally northward flow to the northwest. The eastern reservoir extent appears to be limited by the Aning normal fault that also aligns with the thickening of the clay cap. Given the geologic model, these thickened and deepened conductive zones are more likely to be clay alteration than primary clays of sedimentary origin but further work is required to confirm this.

4.4 Wellbore Scale Permeability

Comparison between well test results and our geologic interpretation revealed that feedzones at Bukit Daun are controlled by both matrix and fracture permeability. The largest feedzones intersected during exploration drilling produce from the Hulusimpang Formation volcanic breccia (~40% of Well-A). The rest of feedzones appear fracture controlled and typically coincide with intervals dominated by relatively N-S striking fractures.

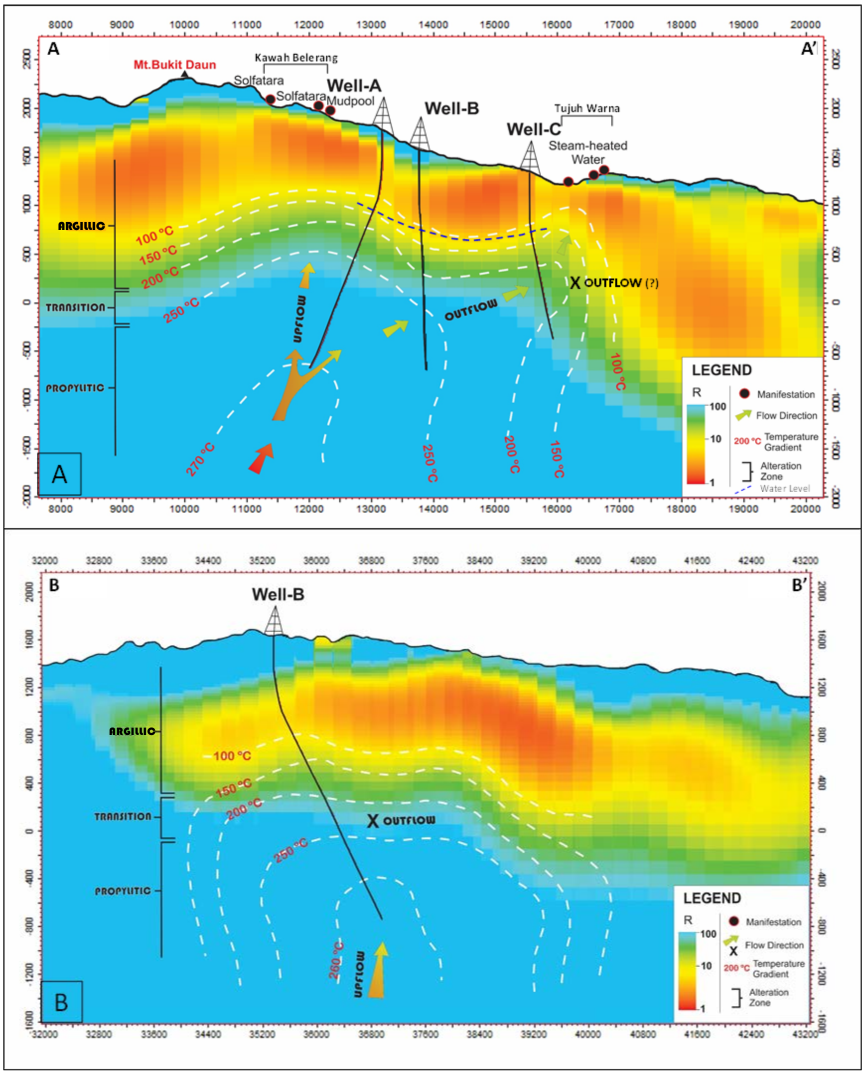

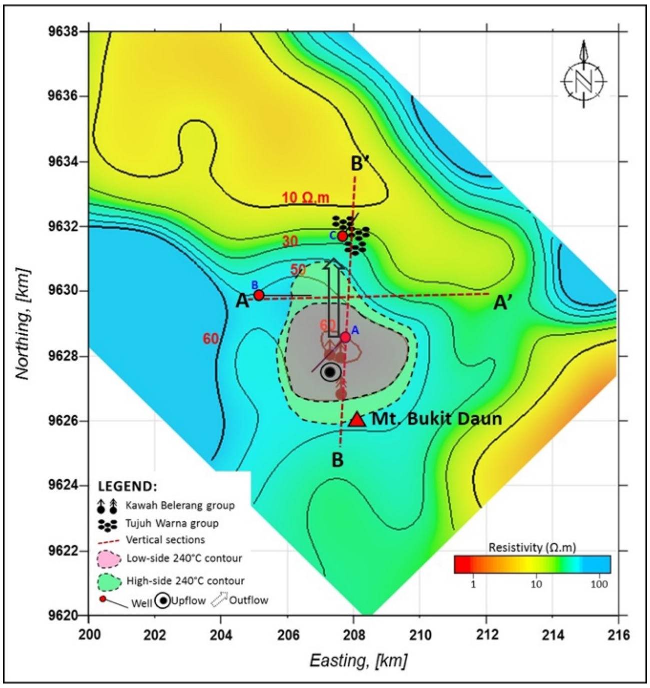

Figure 7: MT cross sections, wells and isotherms on the north-south B-B' line (A) and west-east A-A' line. The temperature isotherms are based on a natural state interpretation of stable well temperature profiles, the shape of the clay cap (i.e., the conductive zone constrained by the MT inversion and plotted here in warm colors), and the system interpretation described in Section 3. (C) A plan view map of Bukit Daun that slices the MT inversion at 0 mRSL, and depicts the well trajectories, flow directions, and cross section lines.

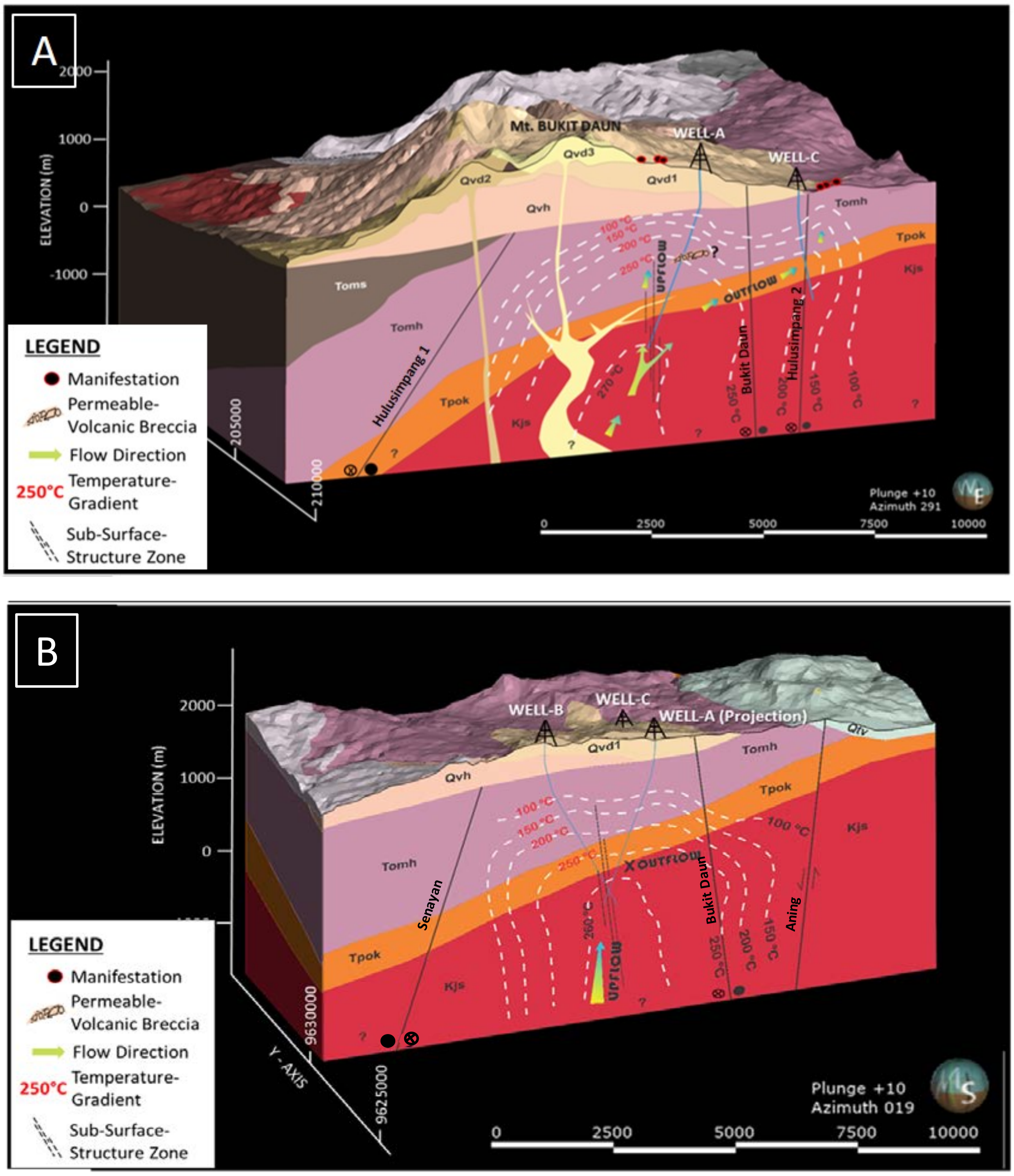

Figure 8: (Upper) Hydrological model of the Bukit Daun geothermal field from A-A' section (see Figure 2 for slice orientation) This section illustrates how fluid flow extends from beneath the Mt. Bukit Daun volcanic center to the Tujuh Warna manifestation. (Lower) The B-B' section (see Figure 2 for slice orientation) shows the inferred width of reservoir, which may be bounded by the Aning normal fault in the east.

5. CONCLUSION

Integration of high-resolution well lithology interpretation with surface mapping and the regional geologic context enabled us to generate a robust model of the structural and stratigraphic context of Bukit Daun geothermal reservoir. This model has improved confidence and plausibility relative to one generated from only well data and the surface geology within the prospect area. The key features of this model include a major unconformity (> 3 ma) where Quaternary volcanic products overly a sequence of Cretaceous to Neogene units that are regionally folded (i.e. tilted). The recent faulting, which is seen cutting Quaternary volcanic products in the terrain images, is consistent with a Riedel simple shear model between regional faults that are parallel to the SFS. Below the unconformity, relic north-trending structures are identified from regional geology and in the borehole image logs. Complex interaction between these relic and modern fault trends may influence the location of the upflow at Bukit Daun.

By combining the geologic model with other resource data, we are able to identify the likely controls on fluid flow at the reservoir and wellbore scale. Our study revealed three possible controls on the outflow direction: (1) north-striking relic faults, perhaps with some interaction with the modern northwest-striking structural regime, (2) the volcanic breccia within the Hulusimpang Formation, and (3) the dip on the Cretaceous to Neogene units that occur at reservoir depth. At the wellbore-scale, feedzones coincide with both matrix (volcanic breccia) and fracture dominated well intervals.

ACKNOWLEDGEMENTS

Muhammad Ikhwan was funded by MFAT of New Zealand Post-graduate Scholarship program. We acknowledge PT. Pertamina Geothermal Energy who provided data and permission to publish this paper. We thank Seequent (Leapfrog Geo) and Schlumberger (Techlog) for use of their software.

REFERENCES

Barber, A. J., Crow, M. J., and Milsom, J., (2005). Sumatra: geology, resources and tectonic evolution. Memoirs of the Geological Society of London, Volume 31, Geological Society of London.

Bellier, O., and Sébrier, M., (1994). Relationship between tectonism and volcanism along the Great Sumatran Fault Zone deduced by SPOT image analyses. Tectonophysics, v. 233, no. 3, p. 215-231.

Bolli, H. M. and Saunders, J. B. (1985). Oligocene to Holocene low latitude planktonic foraminifera. In: H.M. Bolli., J.B. Saunders and K. Perch-Nielsen (eds), Plankton Stratigraphy. Cambridge Univ. Press, 155-262

Darman, H., and Sidi, F. H. (eds.), 2000, An Outline of Geology of Indonesia. Ikatan Ahli Geologi Indonesia, Jakarta.

Cumming, W. (2016). Resource conceptual models of volcano-hosted geothermal reservoirs for exploration well targeting and resource capacity assessment. Proceeding Geothermal Resources Council Annual Meeting, Volume 40, p. 623-637.

Gafoer S., Hermanto, and Amin, T. C. (1992). Geological Map of Indonesia, Bengkulu sheet, Scale 1:250,000. Geological Survey of Indonesia, Geological Research and Development Centre, Bandung.

Ikhwan, M. (2020). Geological Model and Permeability Framework of Bukit Daun Geothermal Field, Indonesia. Unpublished Thesis, Master of Science. School of Environment, University of Auckland, New Zealand.

Kusnama., S., Andi Mangga., and Sukarna. D. (1992). Tertiary stratigraphy and tectonic evolution of southern Sumatra. in Tectonic Framework and Energy Resource of the Western Margin of the Pacific Basin. Proceedings Geological Society of Malay: Circum-Pacific Council for Energy and Mineral Resource, Kuala Lumpur, Malaysia.

Masri, A., Barton, C. A., Hartley, L., and Ramadhan, Y., (2015). Structural permeability assessment using geological structural model integrated with 3D geomechanical study and discrete facture network model in Wayang Windu Geothermal Field, West Java, Indonesia. Proceedings Fourtieth Workshop on Geothermal Reservoir Engineering. Stanford University, Stanford, California.

McCarthy, A., and Elders, C., (1997). Cenozoic deformation in Sumatra: Oblique subduction and the development of the Sumatran Fault System. Geological Society, London, Special Publications, v. 126, no. 1, p. 355-363.

Micklethwaite, S., Ford, A., Witt, W., and Sheldon, H. A., (2015). The where and how of faults, fluids and permeability – insights from fault stepovers, scaling properties and gold mineralisation. Geofluids, v. 15, no. 1-2, p. 240-251.

Moore, G., and Curray, J. (1980). Structure of the Sunda Trench lower slope off Sumatra from multichannel seismic reflection data. Marine Geophysical Researches. v. 4., no. 3, p. 319-340.

Postuma, J. (1971) Manual of Planktonic Foraminifera. Elsevier Publishing Co., Amsterdam, 420.

PT. Pertamina Geothermal Energy Internal Report (2015). Mt. Bukit Daun Geology, Geochemistry and Geophysics Survey Assessment, Unpublished Report, PT. Pertamia Geothermal Energy.

Rickard, W. M., McLennad, J., Islam, N., & Rivas, E. (2019). Mechanical specific energy analysis of the FORGE Utah well. Proceedings Forty-Fourth Workshop on Geothermal Reservoir Engineering, Stanford University, Stanford, California.

Sieh, K., and Natawidjaja, D., (2000). Neotectonics of the Sumatran Fault, Indonesia: Journal of Geophysical Research, Solid Earth, v. 105, no. B12, p. 28295-28326.

Wallis, I.C., Rowland, J. V. and Dempsey, D. E., Allan, G., Sidik, R., Martikno, R., McLean, K., Sihotang, M., Azis, M. and Baroek, M. (this volume) Approaches to imaging feedzone diversity with case studies from Sumatra, Indonesia, and the Taupō Volcanic Zone, New Zealand. Proceedings 42nd New Zealand Geothermal Workshop, Waitangi, New Zealand.

Wallis, I. C., Rowland, J. V., Cumming, W., & Dempsey, D. (2017). The subsurface geometry of a natural geothermal reservoir. Proceedings New Zealand Geothermal Workshop. Rotorua, New Zealand.

Wallis, I. C. McNamara, D. Rowland, J. V. Massiot, C., (2012). The nature of fracture permeability in the basement greywacke at Kawerau Geothermal Field, New Zealand. Proceedings Thirty-Seventh Workshop on Geothermal Reservoir Engineering. Stanford, California.

Yulihanto, B., Situmorang, B., Nurdjajadi, A., & Sain, B. (1995). Structural analysis of the onshore Bengkulu forearc basin and its implication for future hydrocarbon exploration activity. Indonesian Petroleum Association, 24th Annual Convention Proceedings.